doi:10.1016/j.jmb.2004.10.064 J. Mol. Biol. (2005) 345, 339–350

JMB

Available online at www.sciencedirect.com

SCIENCE DIRECT®

ELSEVIER

Caveolin Scaffolding Region and Cholesterol-rich Domains in Membranes

Richard M. Epand[1,2]*, Brian G. Sayer[2] and Raquel F. Epand[1]

[1]*Department of Biochemistry and Biomedical Sciences McMaster University Hamilton, ON, Canada L8N 3Z5*

[2]*Department of Chemistry McMaster University, Hamilton ON, Canada, L8S 4M1*

**Corresponding author*

A protein that constitutes a good marker for a type of cholesterol-rich domain in biological membranes is caveolin. A segment of this protein has a sequence that corresponds to a cholesterol recognition/interaction amino acid consensus (CRAC) motif; this motif has been suggested to cause the incorporation of proteins into cholesterol-rich domains. We have studied the interaction of two peptides containing the CRAC motif of caveolin-1 by differential scanning calorimetry, fluorescence, circular dichroism and magic angle spinning NMR. These peptides promote the segregation of cholesterol into domains from mixtures of the sterol with phosphatidylcholine, as shown by depletion of cholesterol from a portion of the membrane and enrichment of cholesterol in another domain. Cholesterol passes its solubility limit in the cholesterol-rich domain, resulting in the formation of cholesterol crystallites, suggesting that not all of the cholesterol recruited to this domain is bound to the peptide. NMR studies show that the peptides insert somewhat more deeply into membranes when cholesterol is present, but their strongest interaction takes place with the interfacial region of the membrane. We conclude that the peptides we studied containing CRAC sequences are more effective in promoting the formation of cholesterol-rich domains than are shorter peptides of this region of caveolin, which although they contain several aromatic amino acids, they have no CRAC motif. The presence or absence of a CRAC motif, however, is not a sufficient criterion to determine the extent to which a protein will promote the segregation of cholesterol in membranes.

Keywords: caveolae; peptide–lipid interactions; MAS/NMR; cholesterol-rich domain

Introduction

The existence of caveolae in many mammalian cell types has been known morphologically for many years. Caveolae are small structures of 50–100 nm in the plasma membrane that bud inward toward the cell.[1] They are particularly prevalent in adipocytes, endothelial cells and myocytes. Caveolae appear to have a number of functions, including roles in signal transduction[2,3] and lipid recycling.[4,5] Endothelial nitric oxide synthase (eNOS), H-Ras and extracellular signal-regulated kinase (ERK-1/2) appear to be regulated by their interaction with caveolae.[6–8] Caveolae and their constituent proteins, caveolins, have an important role in cardiovascular function, including regulation of nitric oxide synthesis, cholesterol metabolism and cardiac function.[9] The involvement of caveolae in a number of disease processes has been suggested.[10–13]

One of the characteristics of caveolae is the presence of several forms of the protein caveolin.[14,15] Caveolin inserts into membranes of phosphatidylcholine (PC) in a cholesterol-dependent manner.[16] The protein caveolin 1 has particular importance in cholesterol efflux[17] and in binding to intracellular lipid droplets.[18] It has been suggested that the asymmetric binding of caveolae proteins to

Abbreviations used: PC, phosphatidylcholine; PO, 1-palmitoyl-2-oleoyl; SO, 1-stearoyl-2-oleoyl; CRAC, cholesterol recognition/interaction amino acid consensus; DNS-PE, *N*-(5-dimethylaminonaphthalene-1-sulfonyl)-1,2-dihexadecanoyl-*sn*-glycero-3-phosphoethanolamine, triethylammonium salt; MAS, magic angle spinning; MLV, multilamellar vesicle; NOESY, nuclear Overhauser enhancement spectroscopy; LUV, large unilamellar vesicle; SUV, sonicated unilamellar vesicles; DSC, differential scanning calorimetry.

E-mail address of the corresponding author: epand@mcmaster.ca

the membrane can induce membrane bending without involvement of the cytoskeleton.[19] Caveolin-1 has a particular negative regulatory role in signal transduction inhibiting several plasma membrane-initiated signaling cascades[14] and cell growth of embryo fibroblasts in culture. Lung hypercellularity occurs in caveolin-1 knockout mice as a result of endothelial cell hyperplasia.[20,21] Neointimal hyperplasia is an early feature of atherosclerosis[22] and is observed as a result of vascular injury in caveolin-1 deficient mice.[23] It has been suggested recently that caveolin-1 plays an important role in affecting changes in cell morphology that accompany senescence by regulating focal adhesion kinase activity and stress fiber formation.[24]

Caveolae also have a lipid composition rich in cholesterol and sphingomyelin,[25,26] which is similar to lipid "raft" domains in mammalian plasma membranes. The evidence defining caveolae as a cholesterol-rich domain is stronger than for the putative raft domains. The fact that both caveolin and cholesterol are sequestered into the same membrane domain thermodynamically requires that each of these two components will facilitate the sequestering of the other. The system should not be described either as the protein translocating into a lipid domain nor the lipid translocating to bind to the protein, because the interactions are mutual and result in an arrangement exhibiting the lowest free energy, assuming the system is at equilibrium. The modulation of protein-induced domain formation by small changes in lipid composition has been suggested to play an important role in signal transduction.[27] In the case of caveolin, there is another driving force to promote the clustering of the protein into a domain; that is the tendency of caveolin to oligomerize.[28,29]

Caveolin-1 is a 22 kDa protein that is anchored to the membrane with a transmembrane helical segment as well as three sites of palmitoylation at Cys residues. It is common that palmitoylated proteins translocate into cholesterol-rich domains.[30] However, when the three sites of palmitoylation are mutated, the resulting protein still translocates to caveolae.[31] This suggests that segments of the protein itself facilitate the interaction of caveolin-1 with cholesterol-rich domains, although palmitoylation is important for cholesterol binding and transport.[32] Mutational studies indicate that the segment comprising residues 82–101 is necessary and sufficient for membrane binding and has been termed the scaffolding domain.[33] A recent fluorescence microscopy study has shown that a synthetic peptide corresponding to the scaffolding domain of caveolin can recruit NBD-labeled forms of cholesterol and acidic lipids.[34] A consensus sequence, having the pattern -L/V-(X)(1-5)-Y-(X)(1-5)-R/K-, in which (X)(1-5) represents one to five residues of any amino acid, has been found in several proteins that interact with cholesterol.[35] This motif has been termed the CRAC motif as an acronym for cholesterol recognition/interaction amino acid consensus.[36] Caveolin-1 has a segment that corresponds to this consensus sequence. It is residues 94–101 with the sequence VTKYWFYR. A shortened version of this segment that does not fulfil the requirements of the consensus sequence, KYWFYR, was found to sequester the protein to membranes, but is not sufficient to target the protein to the cholesterol-rich domain of caveolae,[37] nor for the blocked synthetic peptide to induce cholesterol-rich domain formation in liposomes.[38] The segment *N*-acetyl-FTVTKYWFYR amide was shown to bind weakly to lipid bilayers in the absence of cholesterol.[39] In the present work, we study the membrane interactions of two longer peptide segments of caveolin that do correspond to the requirements of the consensus sequence described by Li and Papadopolus,[35] i.e. *N*-acetyl-VTKYWFYR amide (residues 94–101) and *N*-acetyl-GIWKASFTTFTVT-KYWFYRL amide (residues 83–102).

Results

Lipid phase separation detected by differential scanning calorimetry (DSC)

We have used DSC analysis to assess the ability of peptides to redistribute lipids into membrane domains. Peptide-induced formation of a cholesterol-rich domain will result in local high concentrations of cholesterol that can exceed the solubility limit of the sterol in membranes, resulting in the formation of cholesterol crystallites.[40] Direct binding of peptides to cholesterol will inhibit the formation of cholesterol crystals, but there is more cholesterol than peptide in the membrane. In addition to binding to cholesterol, the peptide facilitates recruitment of additional cholesterol into a cholesterol-rich domain. As a consequence, cholesterol passes its solubility limit and forms crystals. The fact that cholesterol is recruited to a separate domain is further demonstrated by the depletion of cholesterol from the remainder of the membrane, resulting in a cholesterol-depleted domain that exhibits a more cooperative phospholipid chain melting transition of higher enthalpy. The situation is not unique to caveolin peptides, and has been demonstrated for other cholesterol-binding peptides.[40] A mixture of 1-stearoyl-2-oleoyl phosphatidylcholine (SOPC) and cholesterol at a 6 : 4 molar ratio (Figure 1) and at a 1 : 1 molar ratio (Figure 2), show the formation of anhydrous cholesterol crystallites giving a small endotherm at 36 °C in heating scans and the corresponding exotherm at about 24 °C on cooling. The enthalpy of these cholesterol polymorphic crystalline transitions is summarized in Table 1. Mixtures were run with cholesterol mole fractions of 0.3, 0.4 and 0.5 and a peptide content of 5, 10 or 15 mol% *N*-acetyl-VTKYWFYR amide or 10 mol% *N*-acetyl-GIWKASFTTFTVTKYWFYRL amide. No cholesterol transition was observed at 0.3 mol fraction cholesterol for either peptide (not shown). The transition enthalpy of pure SOPC was reduced from 4000 cal/mol to 1400 cal/mol in the presence

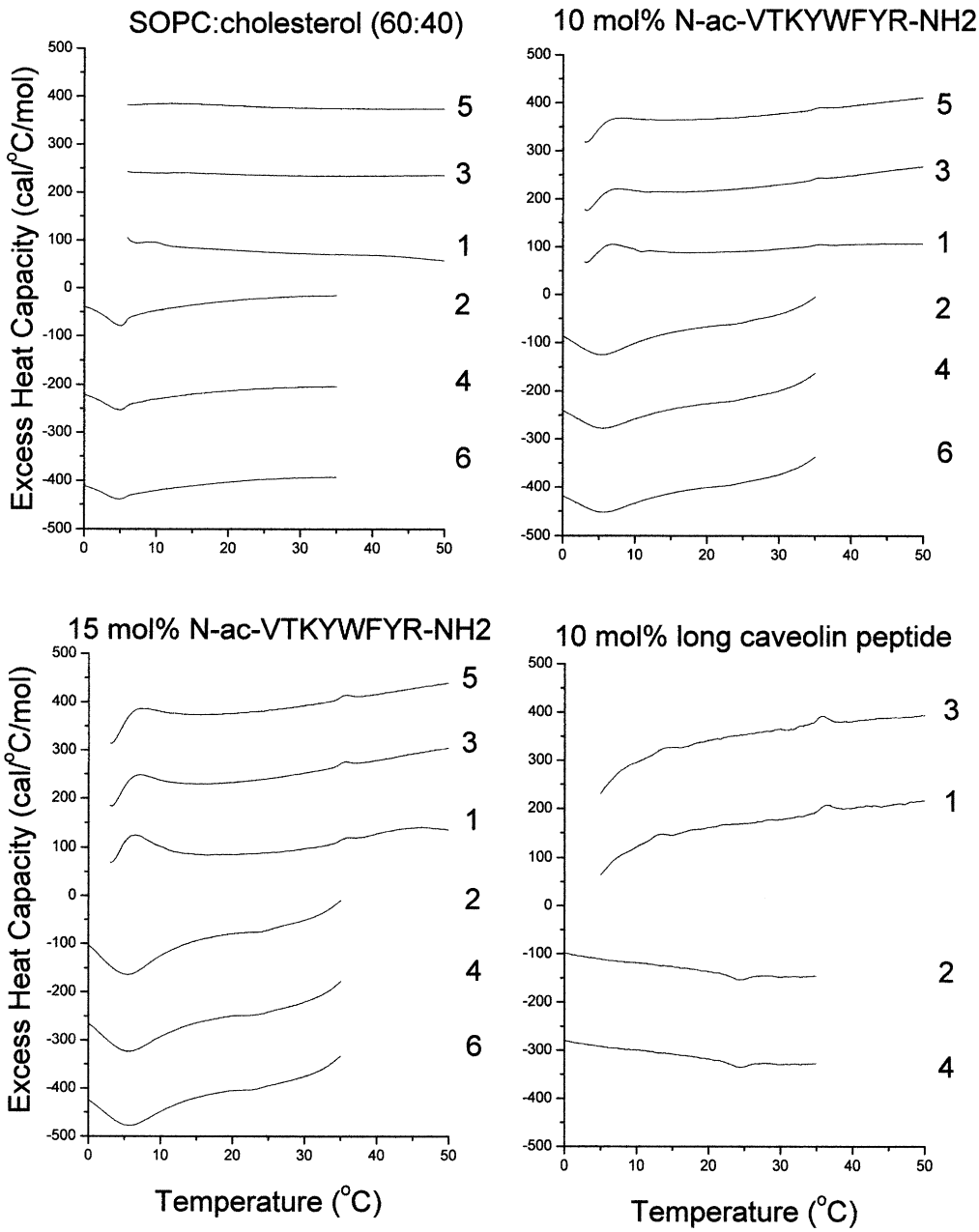

Figure 1. Differential scanning calorimetry of SOPC/cholesterol (6 : 4) and the same lipid mixture with 10 mol% or 15 mol% *N*-acetyl-VTKYWFYR amide or with 10 mol% *N*-acetyl-GIWKASFTTFTVTKYWFYRL amide (long peptide). The scan rate was 2 K/minute. The concentration of lipid was 2.5 mg/ml in 20 mM Pipes (pH 7.40), 1 mM EDTA, 150 mM NaCl, 0.002% (w/v) NaN_3. Sequential heating and cooling scans were between 0 and 50 °C. Numbers are the order in which the scans were carried out, with scans 1, 3 and 5 being heating scans, each of which was followed by one of the cooling scans 2, 4 or 6. Scans are displaced along the *y*-axis for clarity of presentation.

of 10 mol% *N*-acetyl-GIWKASFTTFTVTKYWFYRL amide (1 cal = 4.184 J). In the presence of 30 mol% cholesterol and 10 mol% of this peptide the chain melting transition was too broad to be determined. The enthalpy of this transition in the presence of acetyl-VTKYWFYR amide is summarized in Table 2.

Peptide dissociation from membranes

Although the peptides we are using are hydrophobic and are initially mixed with lipid in organic solvent, we found that another peptide with a CRAC motif, *N*-acetyl-LWYIK amide, dissociated slowly from multilamellar vesicles (MLVs) after hydration.[38] For the peptides used in this study, only the shorter *N*-acetyl-VTKYWFYR amide dissociated partially from the membrane at low concentration (Figure 3). The extent of dissociation of this peptide from lipid is less than what we had found for *N*-acetyl-LWYIK amide; the longer peptide, *N*-acetyl-GIWKASFTTFTVTKYWFYRL amide,

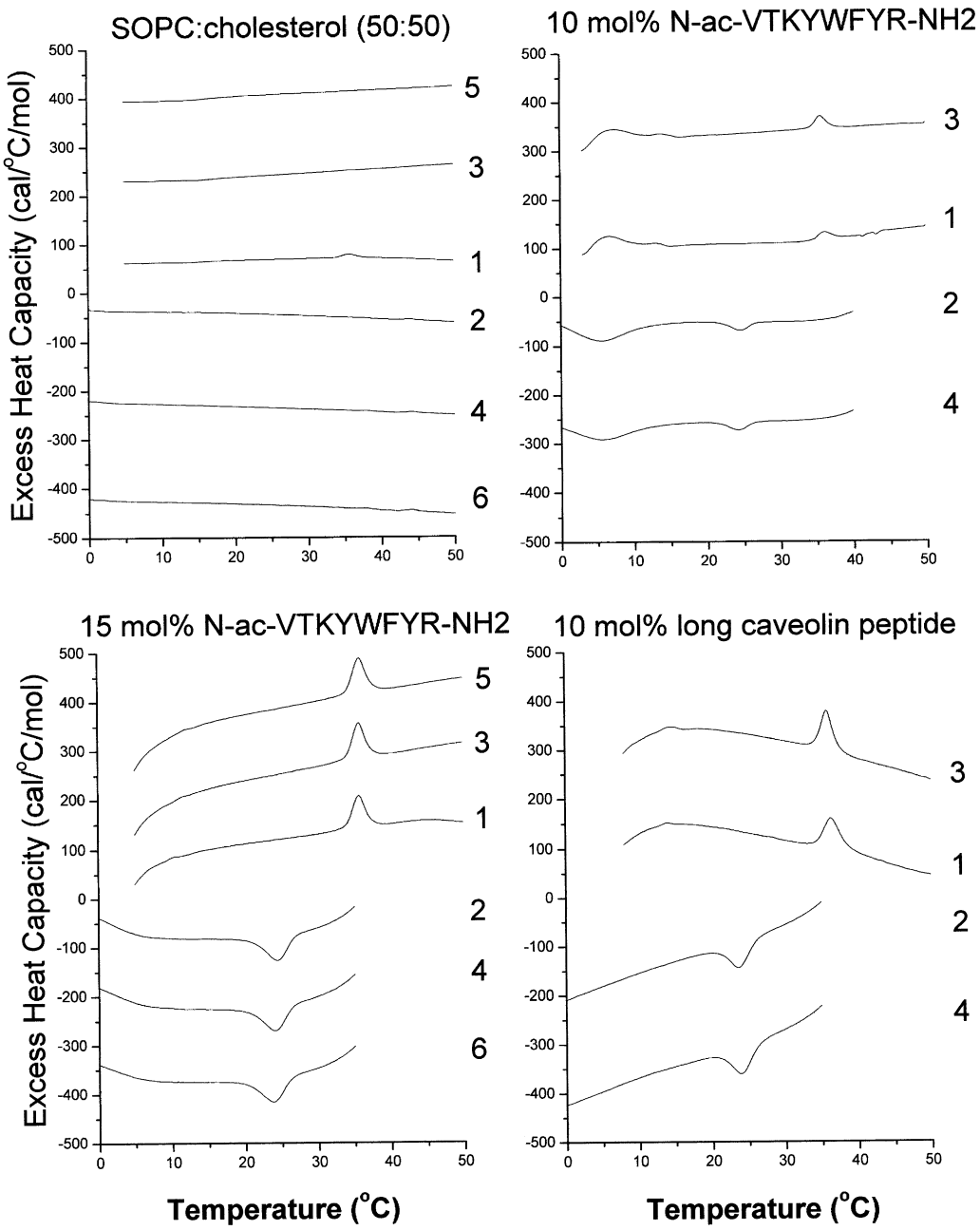

Figure 2. Differential scanning calorimetry of SOPC/cholesterol (1 : 1) and the same lipid mixture with 10 mol% or 15 mol% *N*-acetyl-VTKYWFYR amide or with 10 mol% *N*-acetyl-GIWKASFTTFTVTKYWFYRL amide (long peptide). Other details are as for Figure 1.

Table 1. Formation of anhydrous cholesterol crystals

	% *N*-Acetyl-VTKYWFYR amide			% *N*-Acetyl-GIWKASFTTFTVTKYWFYRL amide
Cholesterol in SOPC (%)	5	10	15	10
40	0	0	15	45
50	38	40	180	210

Values for cholesterol (in cal/mol) were determined from the average area under the transitions at 36 °C on the DSC heating scans corresponding to the polymorphic transition of anhydrous cholesterol crystals.

Table 2. Enthalpy of the chain melting transition of SOPC

Cholesterol in SOPC (%)	*N*-Acetyl-VTKYWFYR amide			
	0	5	10	15
0	4000	3500	4000	2200
40	350	280	350	600

Values for SOPC (in cal/mol) were determined from the average area under the transitions at ~6 °C on the DSC cooling scans, except for pure SOPC in the presence of peptide, where there is a gradual reduction in the transition temperature to 1.4 °C with 15% peptide in cooling scans. Enthalpy values correspond to the liquid crystalline to gel phase transition of the phospholipid on cooling.

did not exhibit any significant dissociation from the membrane (not shown).

Tryptophan fluorescence emission

The fluorescence of the Trp residue(s) have an emission maximum at 339 nm for *N*-acetyl-VTKYWFYR amide and 337 nm for *N*-acetyl-GIWKASFTTFTVTKYWFYRL amide in the presence of 1-palmitoyl-2-oleoyl phosphatidylcholine (POPC). The emission wavelengths of these peptides are similar in the absence of lipid and are shifted about 1 nm to lower wavelengths when adding MLVs containing cholesterol at a POPC/cholesterol molar ratio of 6 : 4. The emission wavelength is insensitive to the peptide to lipid ratio, but the emission intensity decreases with added lipid, particularly for the mixtures of *N*-acetyl-VTKYWFYR amide with POPC/cholesterol (Figure 4). This indicates that the Trp residues of these peptides in water are blue-shifted compared with the usual emission wavelength for Trp in water of ~350 nm. The polarity of the environment does not change much from water when the peptide is mixed with liposomes of either POPC or POPC/cholesterol (1 : 1). There is much less effect of lipid on the emission intensity of these peptides compared with our observations with another peptide with a CRAC sequence, *N*-acetyl-LWYIK amide.[38] A shorter segment from the scaffolding region of caveolin, *N*-acetyl-KYWFYR amide, exhibits similar small effects of lipid on the emission intensity and less change when cholesterol is added to the membrane.[38]

Circular dichroism (CD) of peptides in POPC

The CD spectra of *N*-acetyl-VTKYWFYR amide or *N*-acetyl-GIWKASFTTFTVTKYWFYRL amide in sonicated unilamellar vesicles (SUVs) of POPC indicate that the shorter peptide has little secondary structure, as expected for a short peptide, but the *N*-acetyl-GIWKASFTTFTVTKYWFYRL amide contains some helicity in the presence of SUVs (Figure 5). The CD spectrum of *N*-acetyl-VTKYWFYR amide is largely insensitive to changes in the lipid/peptide ratio between 10 and 100 or for *N*-acetyl-GIWKASFTTFTVTKYWFYRL amide between 100 and 500, suggesting that light-scattering artifacts do not distort the spectra severely. The CD spectrum of *N*-acetyl-VTKYWFYR amide in methanolic solution was similar to that in lipid, indicating that this peptide did not acquire secondary structure even in a helix-promoting solvent.

^{1}H magic angle spinning (MAS) NMR

Static ^{31}P NMR powder patterns demonstrated that all of the samples used for MAS studies were in a bilayer arrangement (not shown). Two-dimensional ^{1}H MAS nuclear Overhauser enhancement spectroscopy (NOESY) spectra were recorded at 25 °C for POPC or POPC/cholesterol (1 : 1), each containing 10 mol% peptide. No resonance assignable to cholesterol was detected.[41] The only resonances that are clearly assignable to the peptide are those of the aromatic protons, in the region 6–8 ppm.[42] The assignments of the lipid ^{1}H chemical shifts are given in Table 3, together with the changes caused by the peptide. The intense peak seen at 4.8 ppm is

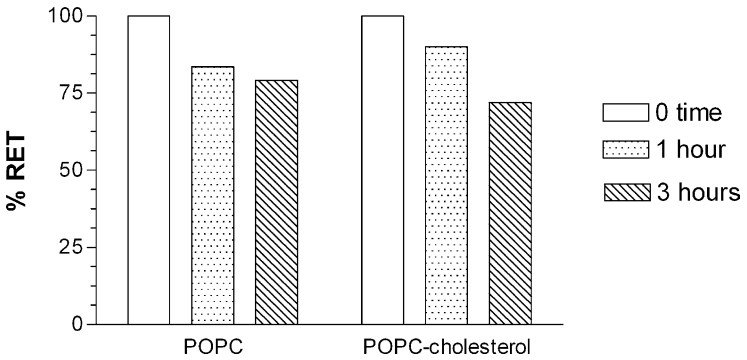

Figure 3. Dissociation at 25 °C of *N*-acetyl-VTKYWFYR amide from liposomes of POPC or of POPC/cholesterol (1 : 1) containing 5 mol% DNS-PE and 10 mol% peptide. The concentration of lipid was 300 μM. Peptide dissociation with time was monitored using the decreased DNS fluorescence emission as a result of loss of energy transfer from the Trp of the peptide at time zero, after one hour and after three hours.

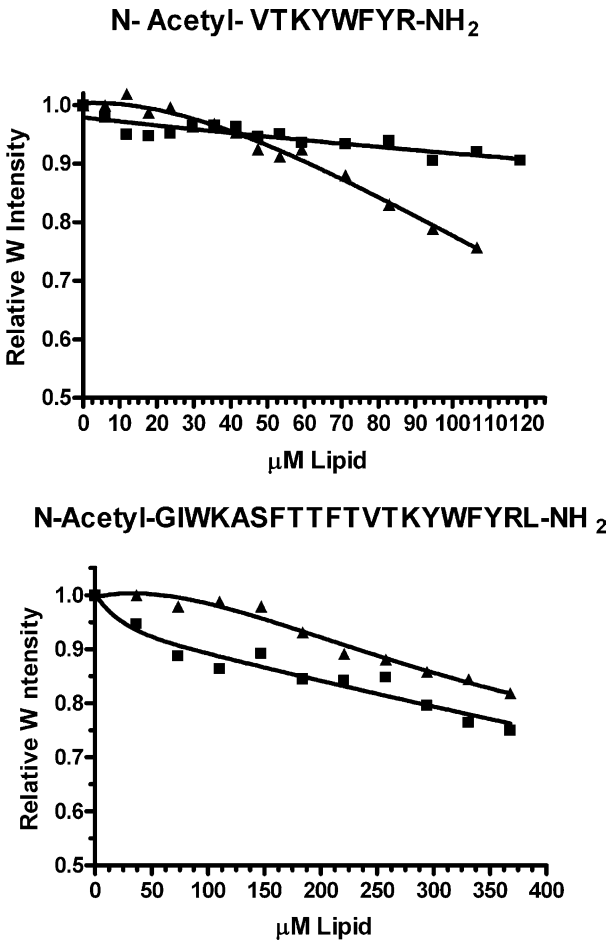

Figure 4. Intensity of fluorescence emission from the Trp (W) residue of *N*-acetyl-VTKYWFYR amide (4.3 μM) and of *N*-acetyl-GIWKASFTTFTVTKYWFYRL amide (2 μM) as a function of the amount of added lipid. (■) POPC; (▲) POPC/cholesterol (6 : 4). The lipid was in the form of MLVs. The excitation wavelength was 295 nm.

caused by residual H_2O that is present in the ^2H_2O. Although the peptide does not cause large changes in the chemical shift, it is only 10 mol% of the lipid, the shifts are significant and suggest that most of the interaction of the peptide is with the lipid headgroup, and that *N*-acetyl-GIWKASFTTFTVTKYWFYRL amide has stronger interactions with the lipid than *N*-acetyl-VTKYWFYR amide. It is interesting that *N*-acetyl-GIWKASFTTFTVTKYWFYRL amide causes a splitting of the peaks from the quaternary CH_3 groups as well as the terminal CH_3 of the acyl chain.

We have focused on NOEs between the aromatic amino acid side-chains and other atoms. The presence of off-diagonal peaks in the 2-D NOESY spectra is indicative of the close approach of two atoms. Slices of the NOESY at the resonance position of the aromatic protons are shown for the spectra of *N*-acetyl-VTKYWFYR amide with POPC (Figure 6) or with equimolar POPC and cholesterol (Figure 7) using mixing times of 50 ms and 300 ms. The longer delay times generally result in larger NOEs by allowing more complete energy transfer through dipolar interactions. However, in the case of POPC with cholesterol in the presence of *N*-acetyl-VTKYWFYR amide, longer delay times result in loss of cross-peak intensity, possibly caused by exchange at the longer time, with peptide that is not membrane-bound. A similar set of NOESY slices is shown for the spectra of *N*-acetyl-GIWKASFTTFTVTKYWFYRL amide with POPC (Figure 8) or with equimolar POPC and cholesterol (Figure 9) using mixing times of 50 ms and 300 ms.

^{13}C chemical shifts exhibit a wider dispersion than those of ^1H and allow for the observation of signals from cholesterol. There are only a few resonances that are shifted by 0.1 ppm or more in the presence of 10% peptide. These are shown in bold in Table 4. Again, it is generally resonances from groups near the membrane interface, and *N*-acetyl-GIWKASFTTFTVTKYWFYRL amide exhibits stronger effects on the lipid in the presence of cholesterol. There is a large change in the chemical shift of the C-18 resonance of cholesterol in the presence of *N*-acetyl-GIWKASFTTFTVTKYWFYRL amide, but this is a consequence of the formation of cholesterol crystallites, as confirmed by DSC.

Discussion

It appears plausible that aromatic amino acid side-chains would facilitate interaction of peptides

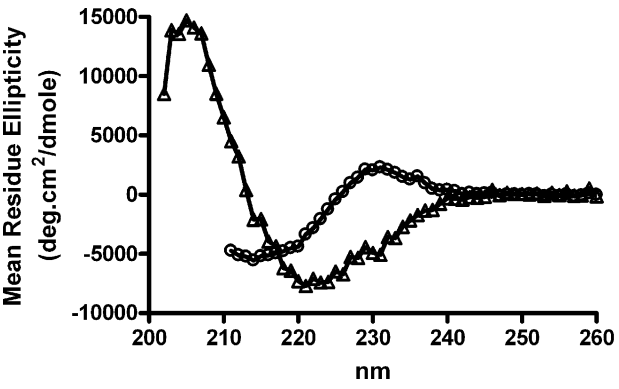

Figure 5. Circular dichroism spectra of *N*-acetyl-VTKYWFYR amide (55 μM) (open circles) and of *N*-acetyl-GIWKASFTTFTVTKYWFYRL amide (6.4 μM) (open triangles) in SUVs of POPC at a lipid to peptide ratio of 100 at 25 °C.

Table 3. ^{1}H NMR chemical shift differences

		Chemical shift difference (ppm)[a]			
		POPC		POPC/cholesterol (1 : 1)	
Resonance	Chemical shift (ppm)	Short	Long	Short	Long
Glycerol C2	5.3	−0.06	−0.04	−0.02	−0.06
Glycerol C3	4.5	−0.02	−0.03	0	−0.06
Choline α	4.3	−0.02	−0.04	−0.01	0.02
Glycerol C1	4.1	−0.04	−0.05	−0.02	−0.01
Choline β	3.7	0	−0.03	0	0.03
Quaternary CH_3	3.3	−0.01	−0.04	0	0.05
Quaternary CH_3	3.3	–	0.02	–	–
CH_2CO	2.4	0	−0.03	0.03	−0.03
CH_2CCO	1.7	−0.01	−0.03	0.01	0.05
CH_2	1.4	−0.02	−0.03	0	−0.03
Terminal CH_3	0.95	−0.03	−0.04	−0.01	−0.03
Terminal CH_3	0.95	–	0.02	–	–

Chemical shifts from 1-D NMR compared with lipid alone. Samples have 10% peptide as either *N*-acetyl-VTKYWFYR amide (Short) or *N*-acetyl-GIWKASFTTFTVTKYWFYRL amide (Long).
[a] Chemical shift difference is calculated as without-with 10% peptide.

with cholesterol, since the planar aromatic ring could stack with the relatively flat structure of cholesterol. However, although the caveolin segment KYWFYR has four successive aromatic amino acid residues, it does not exhibit preferential interaction with cholesterol in mixtures of SOPC and cholesterol,[38] and this segment is not sufficient to target caveolin to the cholesterol-rich domain of caveolae.[37] Lengthening this segment to make *N*-acetyl-VTKYWFYR amide results in a peptide that exhibits some preference for cholesterol-rich domains. It promotes the formation of cholesterol crystals (Table 1) and modestly increases the enthalpy of the SOPC transition in mixtures of SOPC and 40 mol% cholesterol (Table 2). This peptide fulfils the requirements of a CRAC sequence.[35] Thus, the shorter peptide *N*-acetyl-KYWFYR amide, which does not have a CRAC sequence, does not promote the redistribution of cholesterol in the membrane but the longer peptide *N*-acetyl-VTKYWFYR amide, which fulfils the requirement of a CRAC sequence, does promote the formation of cholesterol-rich domains that lead to cholesterol crystallization as well as causing the depletion of cholesterol from other domains in the membrane. It may be that most, if not all, CRAC sequences have some ability to form cholesterol-rich domains, but there are clearly large differences among different peptides with CRAC sequences with regard to their potency. In the present study, the longest peptide, *N*-acetyl-GIWKASFTTFTVTKYWFYRL amide, is more potent in promoting the formation of cholesterol crystals compared with *N*-acetyl-VTKYWFYR amide. The ability of CRAC sequences to promote the formation of cholesterol crystals cannot be a consequence of the peptide

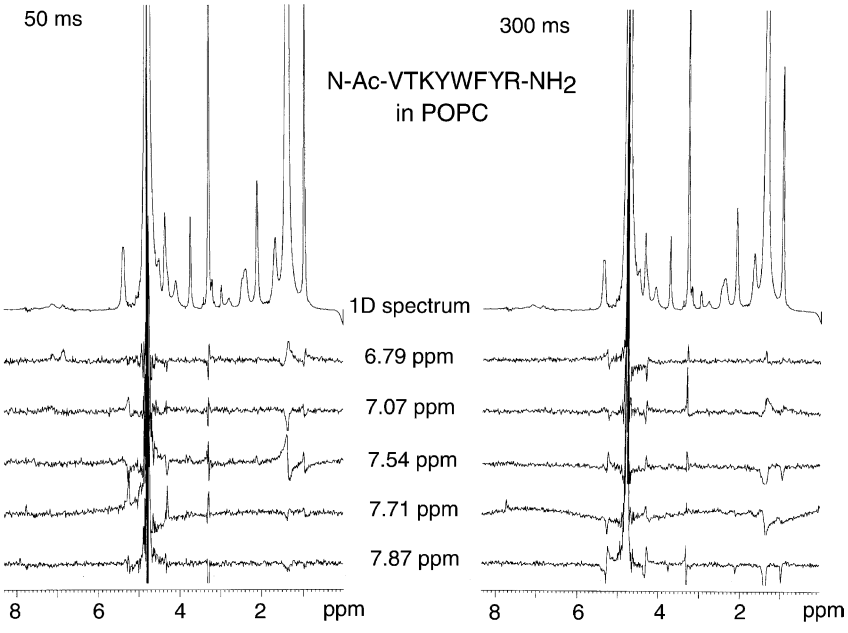

Figure 6. One-dimensional slices from the MAS ^{1}H NOESY spectrum at the chemical shifts of the aromatic protons using mixing times of 50 ms and 300 ms. Spectra are taken from samples of POPC containing 10 mol% *N*-acetyl-VTKYWFYR amide. The top spectra are conventional 1-D proton spectra of the samples.

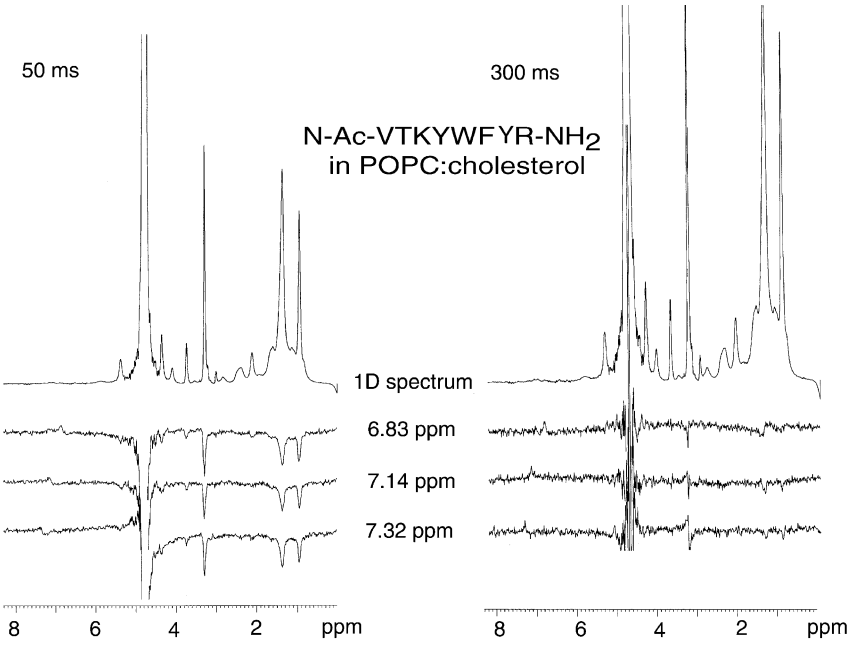

Figure 7. One-dimensional slices from the MAS ^{1}H NOESY spectrum at the chemical shifts of the aromatic protons using mixing times of 50 ms and 300 ms. The spectra are taken from samples of POPC/cholesterol (1 : 1) containing 10 mol% *N*-acetyl-VTKYWFYR amide. The top spectra are conventional 1-D proton spectra of the samples.

binding to cholesterol. Such an interaction would inhibit formation of cholesterol crystals by stabilizing the cholesterol that is bound to the peptide. Apparently, however, the CRAC peptide can alter the properties of the membrane in such a manner as to recruit more molecules of cholesterol to a specific domain, thus passing its solubility limit in the membrane.

The longest peptide does not cause an increase in the chain melting transition enthalpy, likely because this peptide partitions, to some extent, into both cholesterol-rich and cholesterol-depleted domains. This is evidenced also by the fact that this long peptide lowers the transition enthalpy of pure SOPC. Compared with another peptide with a CRAC sequence, *N*-acetyl-LWYIK amide,[38] the two caveolin-related peptides used in this work are less selective in binding to cholesterol-rich domains. Neither of the caveolin peptides causes as great an increase in the enthalpy and cooperativity of the gel to liquid crystalline state phase transition of SOPC as does *N*-acetyl-LWYIK amide.[38] Although, like *N*-acetyl-LWYIK amide, both of the caveolin peptides used in this work show greater penetration into membranes containing cholesterol compared with membranes of pure phosphatidylcholine, the caveolin peptides do not penetrate the membrane as deeply. The strength of the cross-peaks with the acyl chain CH_2 and terminal CH_3 groups are weak, particularly for the shorter of the two caveolin peptides. Most of the cross-peaks with the protons of the aromatic groups

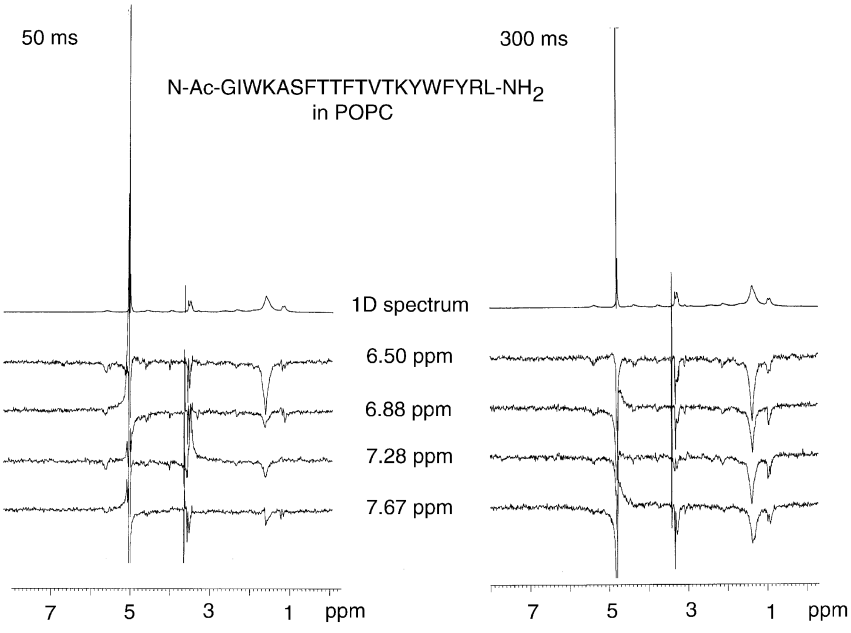

Figure 8. One-dimensional slices from the MAS ^{1}H NOESY spectrum at the chemical shifts of the aromatic protons using mixing times of 50 ms and 300 ms. The spectra are taken from samples of POPC containing 10 mol% *N*-acetyl-GIWKASFTTFTVTKYWFYRL amide. The top spectra are conventional 1-D proton spectra of the samples.

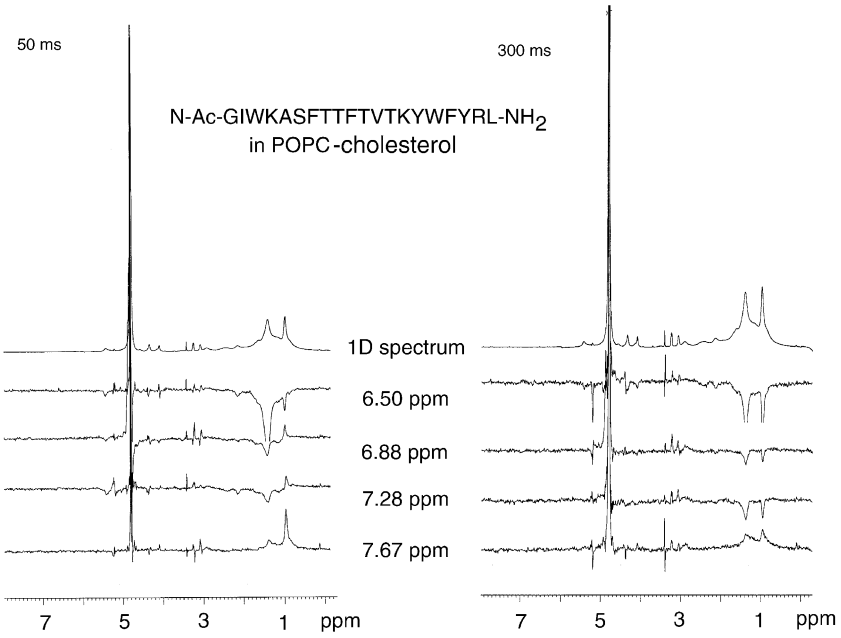

Figure 9. One-dimensional slices from the MAS ^{1}H NOESY spectrum at the chemical shifts of the aromatic protons using mixing times of 50 ms and 300 ms. The spectra are taken from samples of POPC/cholesterol (1 : 1) containing 10 mol% *N*-acetyl-GIWKASFTTFTVTKYWFYRL amide. The top spectra are conventional 1-D proton spectra of the samples.

of the peptide, as well as the peptide-induced changes in the chemical shifts of the resonances from the lipid are with atoms in the headgroup of the lipid. In addition, the lipid has less effect on the Trp fluorescence of the caveolin peptides. Since these peptides do not enter deeply into the membrane, it is likely that their interaction with cholesterol is not very specific. It is possible that the peptide alters the interfacial properties of the membrane so as to favor enrichment of this region of the membrane with cholesterol. Although the caveolin peptides do not insert deeply into membranes, they do translocate efficiently from the aqueous phase to the membrane (Figure 3), so that the lack of sequestering in membranes is not the cause of their weaker potency in segregating cholesterol.

It is likely that in the case of caveolin, the CRAC sequence contributes to binding to caveolae, but this interaction is augmented by other factors. It is known that palmitoylated proteins are generally found in the raft fraction of membranes.[30] Caveolin contains three palmitoyl groups. In addition, there may be interactions or conformations present in the intact protein that are not reproduced in the isolated peptides. In this regard, the CD spectra indicate that the two peptides used in this work have different conformations in membranes (Figure 5), a factor that is likely to contribute to their different effects on the lateral distribution of lipids in the bilayer. The CRAC motif is very general and comprises many possible protein segments. Among the peptides that have been tested, LWYIK appears to be particularly

Table 4. ^{13}C chemical shifts of lipid resonances (ppm)

	POPC			POPC/cholesterol (1 : 1)		
Assignment	No peptide	*N*-acetyl-VTKYWFYR amide	*N*-acetyl-GIWKASFTTF TVTKYWFYRL amide	No peptide	*N*-acetyl-VTKYWFYR amide	*N*-acetyl-GIWKASFTTFTVT-KYWFYRL amide
C=O	173.77	173.83	173.86	173.97	173.95	**174.19/171.77**
Acyl C=C	130.02	130.07	130.01	130.12	130.11	130.05
Acyl C=C	129.65	129.70	129.64	129.62	129.60	129.57
Chol C6	–	–	–	120.69	120.64	120.67
Glycerol C2	71.01	71.04	70.95	71.16	71.09	71.16
Glycerol C3	63.95	**64.15**	**63.42**	64.18	64.19	**64.49**
Choline α	59.83	59.90	59.82	59.92	59.87	**59.32**
$(CH_3)_3+$	54.41	54.44	54.34	54.47	54.40	**56.74**
Chol C9	–	–	–	50.63	50.60	50.58
Chol C13	–	–	–	42.86	42.82	42.84
Chol C24	–	–	–	40.01	39.96	39.96
Chol C1				36.94	36.91	36.79
Acyl C2	34.36	34.43	34.34	34.63	34.57	34.54
Chol C19	–	–	–	19.48	19.42	19.50
Acyl CH_3	14.21	**14.31**	14.19	14.21	14.18	14.15
Chol C18	–	–	–	12.77	**12.66**	**13.12/11.84**

Values of chemical shifts in the presence of peptide, shown in bold, differ from those for the pure lipid by 0.1 ppm or more.

effective in promoting cholesterol segregation. However, it has been pointed out that there are other homologous segments in gp41 proteins of other strains of HIV that do not contain a Tyr and therefore do not formally have a CRAC sequence, yet most likely are also targeted to raft domains.[40] The results of the present study demonstrate that it is not a simple task to identify a raft protein on the basis of the presence of a CRAC sequence, since some of these sequences will be more effective than others in forming a cholesterol-rich domain.

Materials and Methods

Materials

The peptide *N*-acetyl-VTKYWFYR amide was synthesized and purified to >98% purity by HPLC and the peptide *N*-acetyl-GIWKASFTTFTVTKYWFYRL amide were synthesized by Dalton Chemical Laboratories, Toronto, Canada. Phospholipids were purchased from Avanti Polar Lipids (Alabaster, AL), except for the *N*-(5-dimethylaminonaphthalene-1-sulfonyl)-1,2-dihexadecanoyl-*sn*-glycero-3-phosphoethanolamine, triethylammonium salt (DNS-PE) that was purchased from Molecular Probes (Eugene, OR). Cholesterol was purchased from Avanti or from NuChek Prep (Elysian, MN).

Preparation of samples for DSC and NMR experiments

Phospholipid and cholesterol were codissolved in chloroform/methanol (2/1, v/v). For samples containing peptide, an aliquot of a solution of the peptide in methanol was added to the lipid solution in chloroform/methanol. The amount of peptide used was monitored by the absorbance at 280 nm using an extinction coefficient calculated from the amino acid composition.[43] The solvent was then evaporated under a stream of nitrogen with constant rotation of a test-tube so as to deposit a uniform film of lipid over the bottom third of the tube. The last traces of solvent were removed by placing the tube under very reduced pressure for at least two hours. The lipid film was then hydrated with 20 mM Pipes (pH 7.40), 1 mM EDTA, 150 mM NaCl, 0.002% (w/v) NaN_3, and suspended by intermittent vortex mixing and heating to 50 °C over a period of two minutes under argon. Samples used for NMR analysis were hydrated with the same buffer made in ^2H_2O and adjusted to a pH meter reading of 7.0 (pD 7.4) and incubated for at least 24 hours at 4 °C to allow conversion of anhydrous cholesterol crystals to the monohydrate form. For the NMR measurements, the samples were spun in an Eppendorf centrifuge at room temperature. The resulting hydrated pellet was transferred to a 4 mm zirconia rotor with the 12 μl Kel-F insert, attempting to pack the maximal amount of lipid into the rotor while maintaining it wet.

Differential scanning calorimetry (DSC)

Measurements were made using a Nano Differential Scanning Calorimeter (Calorimetry Sciences Corporation, American Fork, UT). The scan rate was 2 °C/minute and there was a delay of five minutes between sequential scans in a series to allow for thermal equilibration. The features of the design of this instrument have been described.[44] DSC curves were analyzed by using the fitting program, DA-2, provided by Microcal Inc. (Northampton, MA) and plotted with Origin, version 5.0.

Large unilamellar vesicles

Lipid films were made as described above for DSC and NMR samples. Films were hydrated with buffer, vortex mixed extensively at room temperature and then subjected to five cycles of freezing and thawing. The homogeneous lipid suspensions were then further processed by ten passes through two stacked 0.1 μm pore size polycarbonate filters (Nucleopore Filtration Products, Pleasanton, CA) in a barrel extruder (Lipex Biomembranes, Vancouver, BC), at room temperature. Large unilamellar vesicles (LUVs) were kept on ice and used within a few hours of preparation. Phosphorus was determined by the method of Ames to obtain the final concentration of lipid.[45]

Dissociation of peptide from membranes by resonance energy transfer

The resonance energy transfer assay between the Trp residue of the peptide and the dansyl group on DNS-PE was used to assess the dissociation of the peptide from a membrane. Lipid films were prepared containing an equimolar mixture of POPC and cholesterol with 5 mol% DNS-PE with or without peptide incorporated into the lipid from methanol solution at a lipid to peptide ratio of 10. The lipid films were hydrated with 10 mM Hepes (pH 7.4), 0.14 M NaCl, 1.0 mM EDTA, to make MLVs and were diluted to a final concentration of 300 μM lipid. The fluorescence emission was measured using an excitation wavelength of 280 nm and a bandwidth of 4 nm in the excitation beam and 8 nm in the emission path. Polarizers, set to 90° in excitation and 0° in emission, were used to reduce stray light. Fluorescence emission spectra were measured using ultrasensitive quartz mirror microcuvettes (N. L. Vekshin, Institute of Cell Biophysics, Pushchino, Russia). Spectra were determined at 25 °C using an SLM Aminco Bowman AB-2 The change of emission intensity at 510 nm was recorded at 37 °C as a function of time. Despite the fact that the peptide had to dissociate from MLVs, rather than LUVs, we observed significant rates of dissociation of some of the peptides. Using MLVs allowed us to avoid extruding the mixture. We use this assay only in a semi-quantitative, comparative manner. In addition, it allows us to have the sample in the same form of MLVs as used for both the DSC and NMR measurements.

Tryptophan fluorescence studies

The peptide was dissolved in 10 mM Hepes (pH 7.4), 0.14 M NaCl, 1.0 mM EDTA. Dilutions were made from a 0.1 mg/ml stock solution. The concentration of peptide was determined by measuring at $A_{280\ nm}$. The excitation wavelength was 295 nm and a bandwidth of 8 nm was used in both excitation and emission. Polarizers, set to 90° in excitation and 0° in emission, were used to reduce stray light. Fluorescence emission spectra were measured using ultrasensitive quartz mirror microcuvettes. Spectra were determined at 25 °C using an SLM Aminco Bowman AB-2 spectrofluorimeter. The spectra were corrected for instrumental factors and a buffer blank was subtracted. Inner filter effect corrections were applied. When the peptide was incorporated into the lipid film, they were then hydrated in Hepes buffer, vortex mixed to make MLVs.

The same concentration of MLVs of lipid without peptide was used as a blank. The concentration of the peptide in the cuvette for all samples was between 2 μM and 4 μM.

Circular dichroism (CD)

The CD spectra were recorded using an AVIV model 61 DS CD instrument (AVIV Associates, Lakewood, NJ). The sample was contained in a 1 mm path-length quartz cell that was maintained at 25 °C in a thermostatically controlled cell-holder. The CD data are expressed as the mean residue ellipticity. Samples for CD were made with peptides codissolved with lipids in methanol and made into a film by solvent evaporation. The film was then suspended by vortex mixing in 10 mM sodium phosphate buffer (pH 7.4) containing 0.14 M NaF and 1 mM EDTA. The suspension was sonicated to clarity to make SUVs. The secondary structure content of the peptides was estimated using the Selcon programme.[46]

^{1}H NOESY MAS NMR

High-resolution MAS spectra were acquired using a 4 mm zirconia rotor with the 12 μl Kel-F insert spinning at 5.5 kHz in a Bruker AV 500 NMR spectrometer. Samples were spun at 5.5 kHz The probe temperature was 24(±1) °C. The 2D-NOESY spectra were obtained using mixing times of 50 ms and 300 ms. Resonances were assigned on the basis of reports of phosphatidylcholine,[41] cholesterol[47] and amino acid residues.[42]

^{13}C Direct Polarization/MAS NMR

A 4 mm zirconia rotor with the 12 μL Kel-F insert was placed in a Bruker Avance 300 spectrometer operating at 75.48 MHz for ^{13}C. The spectra were referenced to an external standard of glycine crystals, assigning a chemical shift of 176.14 ppm for the carbonyl carbon. Samples were spun at 5 kHz. The temperature inside the rotor was 25(±1) °C. Single-pulse excitation with high-power proton decoupling was used with a 4 μs pulse for ^{13}C and the proton frequency optimized for decoupling. A recycle time of five seconds was used.

Acknowledgements

This work was supported by the Canadian Institutes of Health Research grant MT-7654.

References

1. Anderson, R. G. (1998). The caveolae membrane system. *Annu. Rev. Biochem.* **67**, 199–225.
2. Cohen, A. W., Combs, T. P., Scherer, P. E. & Lisanti, M. P. (2003). Role of caveolin and caveolae in insulin signaling and diabetes. *Am. J. Physiol. Endocrinol. Metab.* **285**, E1151–E1160.
3. Chini, B. & Parenti, M. (2004). G-protein coupled receptors in lipid rafts and caveolae: how, when and why do they go there? *J. Mol. Endocrinol.* **32**, 325–338.
4. Fielding, C. J. & Fielding, P. E. (2003). Relationship between cholesterol trafficking and signaling in rafts and caveolae. *Biochim. Biophys. Acta*, **1610**, 219–228.
5. Liu, P., Ying, Y., Zhao, Y., Mundy, D. I., Zhu, M. & Anderson, R. G. (2004). Chinese hamster ovary K2 cell lipid droplets appear to be metabolic organelles involved in membrane traffic. *J. Biol. Chem.* **279**, 3787–3792.
6. Razani, B., Woodman, S. E. & Lisanti, M. P. (2002). Caveolae: from cell biology to animal physiology. *Pharmacol. Rev.* **54**, 431–467.
7. Razani, B. & Lisanti, M. P. (2001). Caveolin-deficient mice: insights into caveolar function human disease. *J. Clin. Invest.* **108**, 1553–1561.
8. Smart, E. J., Graf, G. A., McNiven, M. A., Sessa, W. C., Engelman, J. A., Scherer, P. E. *et al*. (1999). Caveolins, liquid-ordered domains, and signal transduction. *Mol. Cell Biol.* **19**, 7289–7304.
9. Gratton, J. P., Bernatchez, P. & Sessa, W. C. (2004). Caveolae and caveolins in the cardiovascular system. *Circ. Res.* **94**, 1408–1417.
10. Frank, P. G., Woodman, S. E., Park, D. S. & Lisanti, M. P. (2003). Caveolin, caveolae, and endothelial cell function. *Arterioscler. Thromb. Vasc. Biol.* **23**, 1161–1168.
11. Hnasko, R. & Lisanti, M. P. (2003). The biology of caveolae: lessons from caveolin knockout mice and implications for human disease. *Mol. Interv.* **3**, 445–464.
12. Gaudreault, S. B., Dea, D. & Poirier, J. (2004). Increased caveoliN-1 expression in Alzheimer's disease brain. *Neurobiol. Aging*, **25**, 753–759.
13. Simons, K. & Ehehalt, R. (2002). Cholesterol, lipid rafts, and disease. *J. Clin. Invest.* **110**, 597–603.
14. Okamoto, T., Schlegel, A., Scherer, P. E. & Lisanti, M. P. (1998). Caveolins, a family of scaffolding proteins for organizing "preassembled signaling complexes" at the plasma membrane. *J. Biol. Chem.* **273**, 5419–5422.
15. Williams, T. M. & Lisanti, M. P. (2004). The caveolin proteins. *Genome Biol.* **5**, 214.
16. Li, S., Song, K. S. & Lisanti, M. P. (1996). Expression and characterization of recombinant caveolin. Purification by polyhistidine tagging and cholesterol-dependent incorporation into defined lipid membranes. *J. Biol. Chem.* **271**, 568–573.
17. Fu, Y., Hoang, A., Escher, G., Parton, R. G., Krozowski, Z. & Sviridov, D. (2004). Expression of caveolin-1 enhances cholesterol efflux in hepatic cells. *J. Biol. Chem.* **279**, 14140–14146.
18. Robenek, M. J., Severs, N. J., Schlattmann, K., Plenz, G., Zimmer, K. P., Troyer, D. & Robenek, H. (2004). Lipids partition caveolin-1 from ER membranes into lipid droplets: updating the model of lipid droplet biogenesis. *FASEB J.* **18**, 866–868.
19. Sens, P. & Turner, M. S. (2004). Theoretical model for the formation of caveolae and similar membrane invaginations. *Biophys. J.* **86**, 2049–2057.
20. Razani, B., Engelman, J. A., Wang, X. B., Schubert, W., Zhang, X. L., Marks, C. B. *et al*. (2001). Caveolin-1 null mice are viable but show evidence of hyperproliferative and vascular abnormalities. *J. Biol. Chem.* **276**, 38121–38138.
21. Drab, M., Verkade, P., Elger, M., Kasper, M., Lohn, M., Lauterbach, B. *et al*. (2001). Loss of caveolae, vascular dysfunction, and pulmonary defects in caveolin-1 gene-disrupted mice. *Science*, **293**, 2449–2452.
22. Ross, R. (1993). The pathogenesis of atherosclerosis: a perspective for the 1990s. *Nature*, **362**, 801–809.
23. Hassan, G. S., Jasmin, J. F., Schubert, W., Frank, P. G. & Lisanti, M. P. (2004). Caveolin-1 deficiency stimulates neointima formation during vascular injury. *Biochemistry*, **43**, 8312–8321.
24. Cho, K. A., Ryu, S. J., Oh, Y. S., Park, J. H., Lee, J. W.,

Kim, H. P. *et al*. (2004). Morphological adjustment of senescent cells by modulating caveolin-1 status. *J. Biol. Chem.* **279**, 42270–42278.
25. Smart, E. J. & Anderson, R. G. (2002). Alterations in membrane cholesterol that affect structure and function of caveolae. *Methods Enzymol.* **353**, 131–139.
26. Ortegren, U., Karlsson, M., Blazic, N., Blomqvist, M., Nystrom, F. H., Gustavsson, J. *et al*. (2004). Lipids and glycosphingolipids in caveolae and surrounding plasma membrane of primary rat adipocytes. *Eur. J. Biochem.* **271**, 2028–2036.
27. Hinderliter, A., Biltonen, R. L. & Almeida, P. F. (2004). Lipid modulation of protein-induced membrane domains as a mechanism for controlling signal transduction. *Biochemistry*, **43**, 7102–7110.
28. Rothberg, K. G., Heuser, J. E., Donzell, W. C., Ying, Y. S., Glenney, J. R. & Anderson, R. G. (1992). Caveolin, a protein component of caveolae membrane coats. *Cell*, **68**, 673–682.
29. Sargiacomo, M., Scherer, P. E., Tang, Z., Kubler, E., Song, K. S., Sanders, M. C. & Lisanti, M. P. (1995). Oligomeric structure of caveolin: implications for caveolae membrane organization. *Proc. Natl Acad. Sci. USA*, **92**, 9407–9411.
30. Brown, D. A. & London, E. (2000). Structure and function of sphingolipid- and cholesterol-rich membrane rafts. *J. Biol. Chem.* **275**, 17221–17224.
31. Dietzen, D. J., Hastings, W. R. & Lublin, D. M. (1995). Caveolin is palmitoylated on multiple cysteine residues. Palmitoylation is not necessary for localization of caveolin to caveolae. *J. Biol. Chem.* **270**, 6838–6842.
32. Uittenbogaard, A. & Smart, E. J. (2000). Palmitoylation of caveolin-1 is required for cholesterol binding, chaperone complex formation, and rapid transport of cholesterol to caveolae. *J. Biol. Chem.* **275**, 25595–25599.
33. Schlegel, A., Schwab, R. B., Scherer, P. E. & Lisanti, M. P. (1999). A role for the caveolin scaffolding domain in mediating the membrane attachment of caveolin-1. The caveolin scaffolding domain is both necessary and sufficient for membrane binding *in vitro*. *J. Biol. Chem.* **274**, 22660–22667.
34. Wanaski, S. P., Ng, B. K. & Glaser, M. (2003). Caveolin scaffolding region and the membrane binding region of SRC form lateral membrane domains. *Biochemistry*, **42**, 42–56.
35. Li, H. & Papadopoulos, V. (1998). Peripheral-type benzodiazepine receptor function in cholesterol transport. Identification of a putative cholesterol recognition/interaction amino acid sequence and consensus pattern. *Endocrinology*, **139**, 4991–4997.
36. Li, H., Yao, Z., Degenhardt, B., Teper, G. & Papadopoulos, V. (2001). Cholesterol binding at the cholesterol recognition/interaction amino acid consensus (CRAC) of the peripheral-type benzodiazepine receptor and inhibition of steroidogenesis by an HIV TAT-CRAC peptide. *Proc. Natl Acad. Sci. USA*, **98**, 1267–1272.
37. Woodman, S. E., Schlegel, A., Cohen, A. W. & Lisanti, M. P. (2002). Mutational analysis identifies a short atypical membrane attachment sequence (KYWFYR) within caveolin-1. *Biochemistry*, **41**, 3790–3795.
38. Epand, R. M., Sayer, B. G. & Epand, R. F. (2003). Peptide-induced formation of cholesterol-rich domains. *Biochemistry*, **42**, 14677–14689.
39. Arbuzova, A., Wang, L., Wang, J., Hangyas-Mihalyne, G., Murray, D., Honig, B. & McLaughlin, S. (2000). Membrane binding of peptides containing both basic and aromatic residues. Experimental studies with peptides corresponding to the scaffolding region of caveolin and the effector region of MARCKS. *Biochemistry*, **39**, 10330–10339.
40. Epand, R. M. (2004). Do proteins facilitate the formation of cholesterol-rich domains? *Biochim. Biophys. Acta: Bio-Membr.* **1666**, 227–238.
41. Forbes, J., Bowers, J., Shan, X., Moran, L., Oldfield, E. & Moscarello, M. A. (1988). Some new developments in solid-state nuclear magnetic resonance spectroscopy studies of lipids and biological membranes, including the effects of cholesterol in model and natural systems. *J. Chem. Soc., Faraday Trans.* **84**, 3821–3849.
42. Arnold, M. R., Kremer, W., Ludemann, H. D. & Kalbitzer, H. R. (2002). 1H-NMR parameters of common amino acid residues measured in aqueous solutions of the linear tetrapeptides Gly-Gly-X-Ala at pressures between 0.1 and 200 MPa. *Biophys. Chem.* **96**, 129–140.
43. Sober, H. A. (1970). Numerical values of the absorbances of the aromatic amino acids. In *Handbook of Biochemistry: Selected Data for Molecular Biology* (Sober, H. A., ed.), pp. 75–76, The Chemical Rubber Co., Cleveland, OH.
44. Privalov, G., Kavina, V., Freire, E. & Privalov, P. L. (1995). Precise scanning calorimeter for studying thermal properties of biological macromolecules in dilute solution. *Anal. Biochem.* **232**, 79–85.
45. Ames, B. N. (1966). Assay of inorganic phosphate, total phosphate and phosphatases. *Methods Enzymol.* **8**, 115–118.
46. Sreerama, N., Venyaminov, S. Y. & Woody, R. W. (1999). Estimation of the number of alpha-helical and beta-strand segments in proteins using circular dichroism spectroscopy. *Protein Sci.* **8**, 370–380.
47. Guo, W. & Hamilton, J. A. (1996). 13C MAS NMR studies of crystalline cholesterol and lipid mixtures modeling atherosclerotic plaques. *Biophys. J.* **71**, 2857–2868.

Edited by G. von Heijne

(Received 29 July 2004; received in revised form 20 October 2004; accepted 20 October 2004)